

MODELING OF HIGH PRESSURE TURBINE BLADES AND LOW PRESSURE TURBINE BLADES OF AN AEROENGINE THROUGH REVERSE ENGINEERING

Amarjeet Dutta¹, Gaurav Pandey²

¹PG Scholar, Mechanical engineering (CAD/CAM), Axis Institute of Technology and Management, Kanpur, Uttar Pradesh, India

²Assistant Professor, Mechanical engineering (CAD/CAM), Axis Institute of Technology and Management, Kanpur, Uttar Pradesh, India

Abstract- A turbine converts the kinetic energy of hot gases into useful mechanical work. During its operation, hot gases impinge on the turbine blades. Hence, blades are subjected to high thermal fatigue and vibrations, resulting in the development of cracks, occurrence of thermal creep, and mechanical failure. The turbine blades manufactured for aero engines are very costly. Hence, OEM undertakes the repair or refurbishment of the turbine blades. Further, OEM does not always provide the methods of undertaking any maintenance activity on the turbine blades. Hence, this research aims to develop solid models of a High Pressure turbine blade and a Low Pressure turbine blade of an aero engine through reverse engineering. The research involves 3D scanning of blades with a C500 scanner, obtaining data points in STL format and processing with software ezSCAN 2017, converting the point cloud data to a STP file using NX software and developing the solid models from the STP files using Solidworks as the designing software.

Key Words: High pressure (HP), Low pressure (LP), Shrouded, Reverse engineering (RE), 3D scanning, C500, ezSCAN2017, NX, STP, cloud data, Solidworks, offline target positioning, B REP

1. INTRODUCTION

The turbine blades for which modeling is carried out are installed on the turbine of the M53 aero engine. SNECMA¹ defined it as a “single spool and a dual flow military turbopfan aero engine”. It has a modular construction and includes rotors that are supported on three bearings and a frame to support these bearings. The rotating assembly (rotors) is composed of three stages of low pressure axial compressor, five stages of high pressure axial compressor, and two stages of axial turbine. The axial turbine is an assembly of two parts viz. a high pressure turbine and a low pressure turbine. The sequences of the thermodynamic cycle of the engine as described by SNECMA¹ are “intake through the adaptor, compression in the LP (Low Pressure) and HP (High Pressure) compressor, combustion in the combustion chamber, expansion in the turbine, afterburning in AB (After

Burner) duct and exhaust through the exhaust nozzle”. “Air picked up at a certain velocity by the air intake adapter undergoes the first stage of compression in the LP compressor. Part of this after the first stage of compression undergoes the second stage of compression in the HP compressor. It is then channeled to the combustion chamber where it is mixed with atomized fuel and combustion is achieved. The burnt gases then undergo expansion in the turbine. The other part of the air is channeled to the periphery of the engine, mixed with the burnt gases and further combustion is carried out with fuel injected by an afterburner system. The expansion of these burnt gases is continued in a multi-flap exhaust nozzle”.

1.1 Turbine

As per SNECMA¹ the turbine of this aero engine is an “impulse-reaction type which converts the kinetic energy of hot gases into mechanical work for driving the compressor and other components. The HP turbine is made of 84 high pressure blades and the LP turbine is made of 67 low pressure blades”.

1.2 Geometry of HP and LP turbine Blades

The profile of both blades has a pressure face, a suction face, a shrouded tip, and a fir tree type root. The cross-section of the blades has an aerofoil shape. Both the blades are internally hollow to achieve cooling. In addition, holes are provided on the pressure face of the HP blade for additional passage of cooling air.



Fig -1: HP Turbine blade



Fig -2: LP Turbine blade

1.3 Reverse Engineering

Raja and Fernandes¹³ in their book defined reverse engineering as a “process of duplicating an existing part, subassemblies or product without drawing/ documentation or a CAD model”. The general RE process involves three steps:

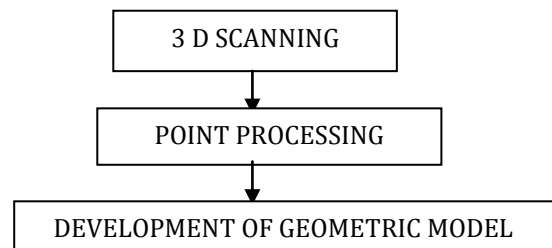


Fig -3: Reverse Engineering

2. METHODOLOGY

During the initial phase of the research, each of a serviceable HP blade and LP blade was identified for developing the respective solid model. Publications provided by the original equipment manufacturer was scrutinised for dimensions of the blades. However, information published in the publications was limited and insufficient to develop solid models. Hence, blades are scanned by C500 optical scanner using blue light technology. The generated data points are processed and validated by ezSCAN2017. The output of the scanning software is a stereolithographic file with .stl format. After validation of the data set, it is converted to a .stp. file by NX software. Finally, this .stp file is used to develop solid models of both the blades using Solidworks.

3. 3D SCANNING

3D optical scanning as defined by Kus⁷ is a “contactless, non-destructive technique” which captures the shape of the turbine blades using blue light technology. This captured image is converted to a digital format by the scanning machine. 3D optical scanner C500 creates “point clouds” of data from the surface of the blades. In other words, the C500 optical scanner captures the blades’ exact size, shape and converts into digital 3-dimensional representation. To obtain the data points from the surface of both the blades, the method used by the C500 scanner is offline target positioning.

4. POINT PROCESSING

The point cloud of both the blades is processed by ezSCAN2017 in two steps: (i) Registration/alignment (ii) Triangulation. In 3D scanning, “all the data points are

brought in to a common reference system and merged into a complete model”, referred as registration by Manor and Fischer¹⁸. Manor and Fischer¹⁸ also described triangulation as the “process of determining the location of a point by measuring angles to it from known points at either end of a fixed baseline”. Polygon models of both the blades are obtained after triangulation.

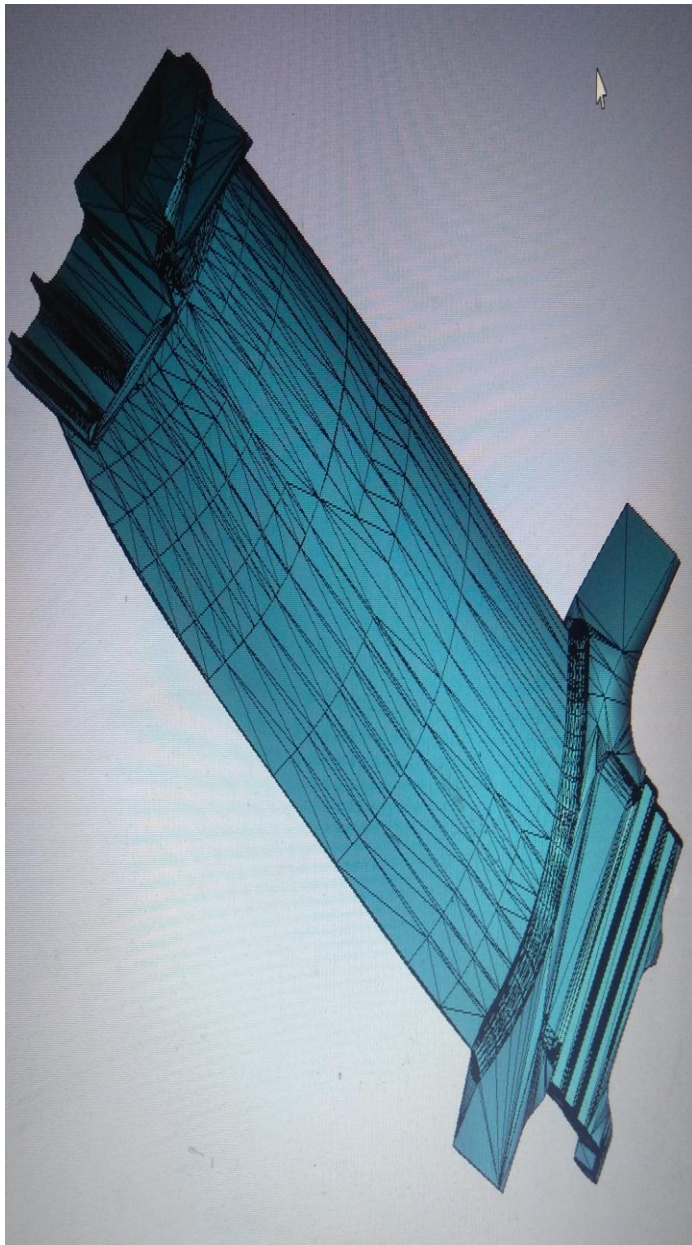


Fig -3: Polygon model of HP blade

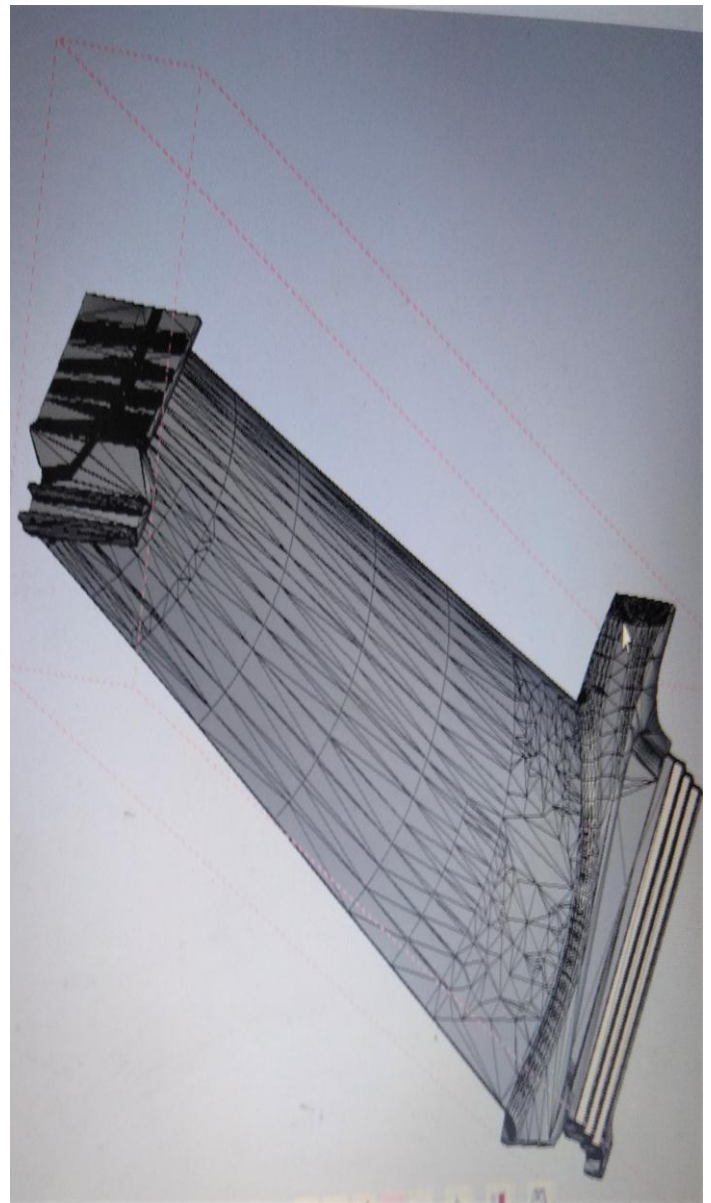


Fig -4: Polygon model of LP blade

5. DEVELOPMENT OF SOLID MODELS

The process followed to develop the solid model is “geometrical reconstruction of the turbine blade” shown by Zhao *et al.*⁶. The reconstruction of the geometry involves conversion of the STL files of HP and LP blades to STP files so that they can be imported to Solidworks. The solid models of both the blades are B REP (Boundary Representation) models. Thompson *et al.*³ in their work described feature based reverse engineering of a mechanical part. In a similar fashion, various curves, surfaces and features are used to develop the models. Rational B Spline curves are extensively used to recreate the aero foil profile of the blades. Zhao *et al.*⁶ in their work showed use of Rational B Spline to develop the shape of a gas turbine blade.



Fig -5: Front view of HP blade

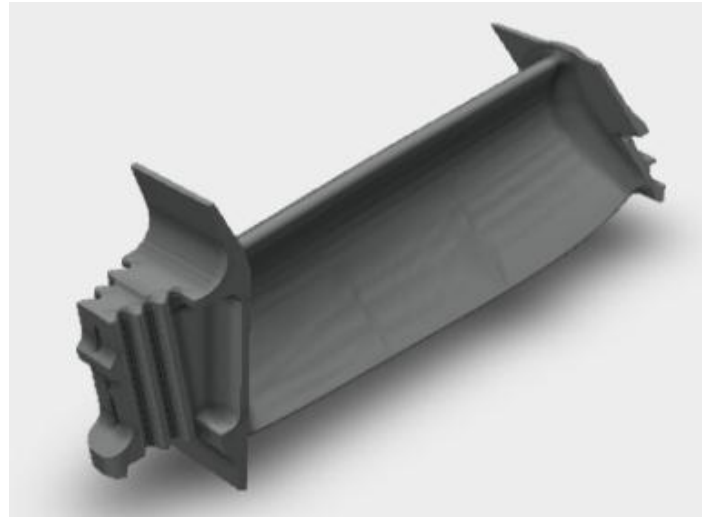


Fig -8: Solid model of HP blade

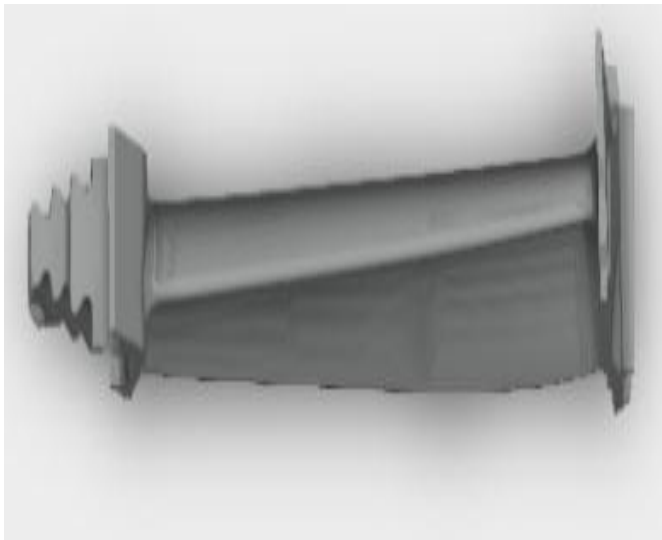


Fig -6: Top view of HP blade



Fig -9: Front view of LP blade

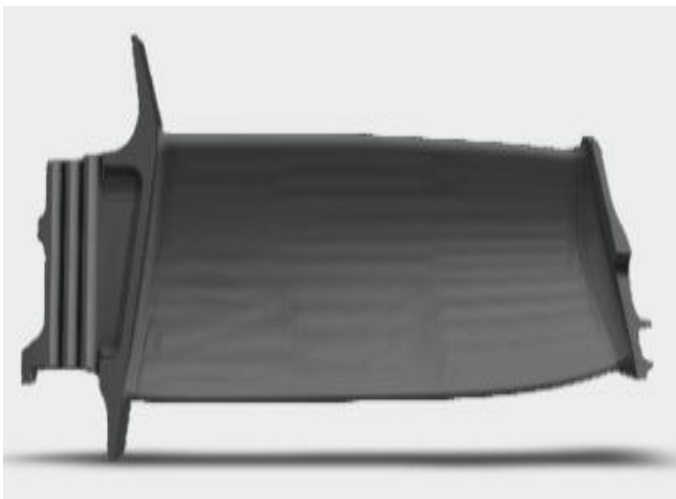


Fig -7: Right view of HP blade



Fig -10: Top view of LP blade



Fig -11: Right view of LP blade



Fig -12: Solid model of LP blade

6. MODELING ENTITIES

The STP files of both the blades are reviewed. After reviewing the STP files, it was inferred that the modeling entities can be grouped into curves, surfaces and features. These entities are used many times during modeling of the blades. These entities are explained in the book by Zeid¹⁴.

6.1 Curves

The basic curves used are lines, circles, ellipses, B splines, B splines with knots, Rational B splines.

6.1.1 Lines

The lines used in modeling of the blades join two coordinate points. Its parametric equation is,

$$\mathbf{P} = \mathbf{P}_1 + u (\mathbf{P}_2 - \mathbf{P}_1), 0 \leq u \leq 1 \quad (1)$$

where, \mathbf{P} = Position vector of an arbitrary point on the line joining points P_2 and P_1 , \mathbf{P}_2 and \mathbf{P}_1 = Position vectors of points P_2 and P_1 respectively, u = a parameter

6.1.2 Circle

The parametric equation of a circle in XY plane can be given by,

$$\begin{aligned} x &= x_c + R \cos u \\ y &= y_c + R \sin u \quad 0 \leq u \leq 2\pi \\ z &= z_c \end{aligned} \quad (2)$$

where, x, y, z are coordinates of an arbitrary point P on the circle, R = radius of the circle, u = the angle measured from x -axis to any point P on the circle, x_c, y_c, z_c are coordinates of the centre of the circle

6.1.3 Ellipse

Ellipse is a curve generated by a point moving in space such that at any position, the sum of its distance from two fixed points (foci) is constant and equal to major diameter. The parametric equation of an ellipse in XY plane is given by,

$$\begin{aligned} x &= x_c + A \cos u \\ y &= y_c + B \sin u \quad 0 \leq u \leq 2\pi \\ z &= z_c \end{aligned} \quad (3)$$

where, x, y, z are coordinates of an arbitrary point P on the ellipse, A = major radius of the ellipse, B = minor radius of the ellipse, u = is the angle measured from x -axis to any point P on the ellipse, x_c, y_c, z_c are coordinates of the centre of the ellipse

6.1.4 B Splines

B spline curve provides local control of the curve shape. It also provides ability to separate the curve degree from the number of data points that defines it. This achieved through basis functions known as B spline. The parametric equation of B spline is given by,

$$\mathbf{P}(u) = \sum_{i=1}^n \mathbf{P}_i N_{i,k}(u) \quad 0 \leq u \leq u_{max} \quad (4)$$

where, $\mathbf{P}(u)$ = Position vector of a point on B Spline curve, $N_{i,k}(u)$ = B Spline function, k = a parameter controlling the degree of B Spline curve, u = a parameter

6.1.5 B Splines with knots

The nature of this curve is same as B Spline and mathematically defined by Equation 4 but with a knot vector defined as

$$\mathbf{KV} = [u_0, u_1, u_2, \dots, u_v]^T \quad (5)$$

6.1.6 Rational B Spline

A rational B Spline curve defined by $n+1$ control points P_i is given by,

$$\mathbf{P}(u) = \sum_{i=1}^n P_i R_{i,k}(u) \quad 0 \leq u \leq u_{max} \quad (6)$$

where, $\mathbf{P}(u)$ = Position vector of a point on B Spline curve, $R_{i,k}(u)$ = B Spline function, k = a parameter controlling the degree of Rational B Spline curve, u = a parameter,

Rational B Spline function is defined as,

$$R_{i,k}(u) = \frac{w_i N_{i,k}(u)}{\sum_{i=1}^n w_i N_{i,k}(u)} \quad (7)$$

where, w_i = weights associated with control points P_i of Rational B Spline

6.2 Surfaces

Some of the surfaces used to model the blades are plane, cylindrical surface and B spline surface with knots.

6.2.1 Plane

The parametric equation of a plane surface passing through three points P_0, P_1 and P_2 is given as,

$$\mathbf{P}(u,v) = \mathbf{P}_0 + u(\mathbf{P}_1 - \mathbf{P}_0) + v(\mathbf{P}_2 - \mathbf{P}_0) \quad (8)$$

$0 \leq u \leq 1, 0 \leq v \leq 1$

where, \mathbf{P} = Position vector of an arbitrary point on the plane, P_0, P_1 and P_2 = Position vectors of points respectively, u and v are parametric dimensions

6.2.2 Cylindrical surface

A cylindrical surface results from translating a planar curve along a given direction. The position vector of any point $P(u,v)$ on the surface can be given by,

$$\mathbf{P}(u,v) = \mathbf{G}(u) + \mathbf{n}_v \quad (9)$$

$0 \leq u \leq u_{max}$
 $0 \leq v \leq v_{max}$

where, $\mathbf{G}(u)$ is an existing curve to create the cylinder, v =cylinder length, \mathbf{n}_v = cylinder axis

6.2.3 B Spline surface with knots

A B Spline surface defined by $(n+1) \times (m+1)$ array of control points is given by,

$$\mathbf{P}(u,v) = \sum_{i=0}^n \sum_{j=0}^m P_{ij} N_{i,k}(u) N_{j,l}(v) \quad (10)$$

$0 \leq u \leq u_{max}$
 $0 \leq v \leq v_{max}$

where, $\mathbf{P}(u,v)$ = position vector of an arbitrary point P on the surface, P_{ij} = control points of the surface, $(n+1) \times (m+1)$ is rectangular array of control points, k and l are knot vectors in the direction u and v respectively, $N_{i,k}(u)$ and $N_{j,l}(v)$ = basis functions

6.3 Features

Zeid¹⁴ defined feature as a shape and operation to build parts. The shape is a two dimensional sketch. The operation is an activity that converts the sketch into three dimensional shapes. Features used during modeling of blades are briefly explained in subsequent sub- sections.

6.3.1 Extrusion

It is used to create a uniform thickness model. An extrusion vector and a cross- section are required to perform extrusion.

6.3.2 Draft

Draft is used to create taper in model faces. To perform draft operation, a draft angle and a face is required.

6.3.3 Revolve

This feature performs the function of creating axi-symmetric solids. An axis of revolution, a cross-section and an angle of revolution is required to perform this operation.

6.3.4 Holes

This feature is used to create holes in the model. It requires a diameter, a length and axis to define orientation.

6.3.5 Fillets and chamfer

Fillet rounds the corners of a model. A chamfer creates transition between two edges of a model.

7. ANALYSES AND RESULTS OF SOLID MODELING

Analysing the models of both the blades is carried out to check errors and establish validity of the models. Analyses carried out on the models are geometry analysis, thickness analysis, deviation analysis and draft analysis.

7.1 GEOMETRY ANALYSIS

Geometry analysis identifies geometric entities in the models of the blades that could cause errors in other applications such as CAM. Entities that are identified during analysis are sliver faces, small faces, short edges, sharp (knife) edges and vertices, discontinuous edges and faces.

Table -1: Faces and edges in HP blade

Entity Type	No. of Entities
Short edges	29
Small faces	1
Sliver faces	10
Knife edges	0
Knife vertices	2
Discontinuous faces	0
Discontinuous edges	0

Table -2: Faces and edges in LP blade

Entity Type	No. of Entities
Short edges	25
Small faces	1
Sliver faces	6
Knife edges	0
Knife vertices	10
Discontinuous faces	0
Discontinuous edges	0

7.2 THICKNESS ANALYSIS

Thickness analysis is carried out to determine thickness at various sections of the blades. It serves the purposes of identify thick and thin region, determine portion of a part that are equal to specified target thickness, identify design flaws.

Table -3: Summary of thick thickness analysis of HP blade

Total surface area analyzed	13314.91 mm ²
Critical surface area (% of analyzed area)	5907.14 mm ² (44.36%)
Maximum deviation from target thickness	3 mm
Average weighted thickness on critical area	4.49 mm
Average weighted thickness on analyzed area	6.19 mm
Number of critical faces	232 Face(s)
Number of critical features	1
Minimum thickness on analyzed area	0.02 mm
Maximum thickness on analyzed area	119.8 mm

Table -4: Thick thickness analysis details of HP blade

Thickness range	Number of faces	Surface area	% of analyzed area
3 mm to 3.75 mm	36	1532.55 mm ²	11.51
3.75 mm to 4.5 mm	22	1385.51 mm ²	10.41
4.5 mm to 5.25 mm	50	1632.47 mm ²	12.26
5.25 mm to 6 mm	124	1356.6 mm ²	10.19

Table -5: Summary of thin thickness analysis of HP blade

Total surface area analyzed	13314.91 mm ²
Critical surface area(% of analyzed area)	4277.67mm ² (32.13%)
Maximum deviation from target thickness	2.98 mm
Average weighted thickness on critical area	2 mm
Average weighted thickness on analyzed area	6.19 mm
Number of critical faces	208 Face(s)
Number of critical features	1
Minimum thickness on analyzed area	0.02 mm
Maximum thickness on analyzed area	119.8 mm

Table -6: Thin thickness analysis details of HP blade

Thickness range	Number of faces	Surface area	% of analyzed area
3 mm to 2.25 mm	42	1534.96 mm ²	11.53
2.25 mm to 1.51 mm	83	1709.02 mm ²	12.84
1.51 mm to 0.76 mm	59	953.31 mm ²	7.16
0.76 mm to 0.02 mm	24	80.37 mm ²	0.60

Table -7: Summary of thick thickness analysis of LP blade

Total surface area analyzed	21055.12 mm ²
Critical surface area(% of analyzed area)	8271.14 mm ² (39.28%)
Maximum deviation from target thickness	3 mm
Average weighted thickness on critical area	4.63 mm
Average weighted thickness on analyzed area	7.55 mm
Number of critical faces	231 Face(s)
Number of critical features	1
Minimum thickness on analyzed area	0.06 mm
Maximum thickness on analyzed area	179.62 mm

Table -8: Thick thickness analysis details of LP blade

Thickness range	Number of faces	Surface area	% of analyzed area
3mm to 3.75mm	28	1716.82 mm ²	8.15
3.75mm to 4.5mm	23	1808.55 mm ²	8.59
4.5mm to 5.25mm	43	2217.42 mm ²	10.53
5.25mm to 6mm	137	2528.34 mm ²	12.01

Table -9: Summary of thin thickness analysis of LP blade

Total surface area analyzed	21055.12 mm ²
Critical surface area(% of analyzed area)	4710.81mm ² (22.37%)
Maximum deviation from target thickness	2.94 mm
Average weighted thickness on	1.97 mm

critical area	
Average weighted thickness on analyzed area	7.55 mm
Number of critical faces	187 Face(s)
Number of critical features	1
Minimum thickness on analyzed area	0.06 mm
Maximum thickness on analyzed area	179.62 mm

Table -10: Thin thickness analysis details of LP blade

Thickness range	Number of faces	Surface area	% of analyzed area
3mm to 2.27mm	66	1465.17 mm ²	6.96
2.27mm to 1.53mm	66	2284.67 mm ²	10.85
1.53mm to 0.8 mm	41	766.28 mm ²	3.64
0.8mm to 0.06mm	14	194.69 mm ²	0.92

5.3 DEVIATION ANALYSIS

It calculates angle between faces. Here, maximum, minimum and average deviation is shown for HP and LP blade.

Table -11: Deviation analysis of HP blade

Deviation	Value
Maximum	106.38°
Average	7.41°
Minimum	0°

Table -12: Deviation analysis of LP blade

Deviation	Value
Maximum	106.38°
Average	7.41°
Minimum	0°

5.4 DRAFT ANALYSIS

Draft analysis checks draft angles of various faces in the blades. Here, positive draft, negative draft, straddle faces, positive steep faces and negative steep faces are shown for both blades.

Table -13: Draft analysis of HP blade

Draft	No. of faces
Positive	126

Negative	73
Straddle faces	129
Positive steep faces	21
Negative steep faces	6

Table -13: Draft analysis of LP blade

Draft	No. of faces
Positive	81
Negative	59
Straddle faces	122
Positive steep faces	40
Negative steep faces	29

8. CONCLUSIONS

Designing of the blades through reverse engineering requires that performance of the blades should improve. Hence, any research on blades through reverse engineering should improve the geometrical design of the blades. This research paper specifically addresses the need of having solid models of LP and HP blades to undertake any repair or refurbishment activity on turbine of M53 aero engine. The dimensions of the blades not provided by OEM are also found out during the study. The .stp file of both blades stipulates every detail required to remake the models and provides a window to further improve the design of the blades which would address the current defects such as cracks and creep. This research would serve as a guideline for developing new repair and maintenance technologies. It would also serve as a guideline for further development of turbine blade models.

REFERENCES

- [1] SNECMA. "Overhaul of stage 1 and stage 2 discs". Safran engines, no.3 (2017).
- [2] K. Mohaghegh, M.H. Sedeghi and A.A. Abdullah. "Reverse engineering of turbine blades on design intent". International Journal of Advanced Manufacturing Technology, no.32 (2007): 1009-1020.
- [3] William B. Thompson, Jonathen C. Owen, H. James de St. Germain, Stevan R. Stack Jr. and Thomas C. Henderson. "Feature based reverse engineering of mechanical parts". IEEE Transactions on Robotics and Automation, no.15 (1999): 1042-296X.
- [4] A. Gameros, L. de Chiffre, H.R. Siller, J. Hiller and G. Genta. "A reverse engineering methodology for nickel alloy turbine blades with internal features". CRIP Journal of

Manufacturing Science and Technology, no. 299 (2014):1755-5817.

[5] K. Ravindra and P. V. Dinakar Raju. "Modeling and analysis of gas turbine rotor blade". International Research Journal of Engineering and Technology, no.4 (2017): 2395-0056.

[6] Zhengcai Zhao, Yucan Fu, Xuan Liu, Jiuhua Xu, Jun Wang, Sujie Mao. "Measurement based geometric reconstruction for milling turbine blade using free form deformation". Elsevier, no. 101 (2017): 19-27.

[7] Abdil Kus. "Implementation of 3D optical scanning technology for automotive application". www.mdpi.com/journal/sensors, no.9 (2009).

[8] John T. Pickens. "Reverse engineering method for disc and blade attachment". United States Patents, no. US7,720,699B2 (2010).

[9] Alexander Stankowski, Lukas Emanuel Rickenbacher and Simone Hövel. "Method for repairing and/or upgrading a component of a gas turbine". United States Patent Application Publication, no. US2011/0264413A1 (2011).

[10] Irwin E. Treager. "Aircraft gas turbine engine technology". www.scribd.com/document/320166637.

[11] Meherwan P. Boyce. "Gas turbine engineering handbook". Elsevier. Inc. 2012.

[12] Gaurav Varma and Matt Weber. "SolidWorks 2020 Black Book, CAD/CAM/CAE Works,2019.

[13] Vinesh Raja, Kiran J. Fernandes. "Reverse Engineering- An Industrial Perspective". Springer Science and Business Media, 2008.

[14] Ibrahim Zeid. "Mastering CAD/CAM". Tata Mc- Graw Hill, 2005.

[15] P.K. Nag. "Power plant engineering." McGraw Hill Education Pvt. Ltd, 2014.

[16] R.K. Rajput. "Internal combustion engines." Laxmi Publication Ltd, 2008.

[17] Sansagith. "3Dscanning". www.scribd.com

[18] A. Manor and A. Fischer. "Reverse engineering of 3D models based on image processing and 3D techniques". CMSR Laboratory for Computer Graphics and CAD, 2017.

[19] Point cloud conversion to 3D modeling. www.scribd.com/document/421676825.

[20] C500 Solutionx Scanners, Exact Dimensions.

